

¹ Centre for Ecology and Hydrology, Wallingford, U.K.

² Hadley Centre for Climate Prediction and Research, Met Office, Exeter, U.K.

³ Ecology and Resource Management, School of GeoSciences, University of Edinburgh, Edinburgh, U.K.

⁴ Instituto Nacional de Pesquisas da Amazonia, Manaus, Amazonas, Brazil

Calibration of a land-surface model using data from primary forest sites in Amazonia

P. P. Harris¹, C. Huntingford¹, J. H. C. Gash¹, M. G. Hodnett¹, P. M. Cox², Y. Malhi³, and A. C. Araújo⁴

With 7 Figures

Received March 27, 2003; revised October 23, 2003; accepted November 3, 2003

Published online April 28, 2004 © Springer-Verlag 2004

Summary

A land-surface model (MOSES) was tested against observed fluxes of heat, water vapour and carbon dioxide for two primary forest sites near Manaus, Brazil. Flux data from one site (called C14) were used to calibrate the model, and data from the other site (called K34) were used to validate the calibrated model. Long-term fluxes of water vapour at C14 and K34 simulated by the uncalibrated model were good, whereas modelled net ecosystem exchange (NEE) was poor. The uncalibrated model persistently underpredicted canopy conductance (g_c) from mid-morning to mid-afternoon due to saturation of the response to solar radiation at low light levels. This in turn caused a poor simulation of the diurnal cycles of water vapour and carbon fluxes. Calibration of the stomatal conductance/photosynthesis sub-model of MOSES improved the simulated diurnal cycle of g_c and increased the diurnal maximum NEE, but at the expense of degrading long-term water vapour fluxes. Seasonality in observed canopy conductance due to soil moisture change was not captured by the model. Introducing realistic depth-dependent soil parameters decreased the amount of moisture available for transpiration at each depth and led to the model experiencing soil moisture limitation on canopy conductance during the dry season. However, this limitation had only a limited effect on the seasonality in modelled NEE.

1. Introduction

Many studies have shown that modelled land-surface fluxes exert a strong influence on the climate simulated by global circulation models (GCMs; Garratt, 1993). As a result, land-surface parameterisations have evolved from simple descriptions involving globally uniform albedo, roughness length and stomatal conductance to more complex and realistic soil-vegetation-atmosphere transfer (SVAT) schemes. These models have provided useful tools for assessing the potential impact of land-surface change on climate. For example, numerous GCM studies have assessed the impact of large-scale deforestation in Amazonia (Dirmeyer and Shukla, 1994; Polcher, 1995; Lean et al., 1996) and found significant modification of climate both locally and remote to the land-surface change.

More recent work has shown that the converse is also true, in that modelled vegetated land cover is sensitive to climate. White et al. (1999) forced a dynamic vegetation model (Hybrid; Friend et al., 1997) with a GCM climate simulated

under increasing greenhouse gas emissions. They found that large areas of the modelled Amazonian rainforest changed to savanna or desert by the year 2080. Friedlingstein et al. (2001) demonstrated that change in the rate of carbon uptake by the terrestrial biosphere has the potential to amplify climate change by increasing the rate at which CO₂ accumulates in the atmosphere. Cox et al. (2000) ran simulations using a coupled atmosphere-ocean GCM including a closed carbon cycle with dynamic vegetation forced by increasing anthropogenic greenhouse gas emissions – thus allowing for feedbacks between climate and the carbon cycle. This model experiment also resulted in the replacement of Amazonian rainforest by grassland and desert, and subsequent acceleration of anthropogenically induced climate change. Elsewhere in this issue, Cox et al. (2004) and Betts et al. (2004) present further analysis of this experiment with respect to Amazonia. Betts et al. demonstrate that physiological, biogeographical and biogeochemical feedbacks between the Amazonian land-surface and climate contribute to approximately 50% of the modelled future precipitation reduction in this region.

These studies highlight the importance of integrating the carbon cycle into GCM simulations of future climate. But in doing so it is also important that the ability of different GCM components (such as the land-surface scheme) to simulate present conditions is tested against observations. Computational limitations require that these tests be carried out with the land-surface scheme off-line from the GCM (Delire and Foley, 1999). In this paper Version 2 of the Met Office Surface Energy Scheme (MOSES, Cox et al., 1999) is tested and calibrated against carbon dioxide and water vapour flux data from two primary rainforest sites near Manaus, Brazil.

2. Sites and data

Field measurements were used from two primary rainforest sites, called C14 and K34, in the Reserva Biológica do Cuieiras (a forest reserve belonging to Instituto Nacional de Pesquisas da Amazonia, INPA), located roughly 60 km north of Manaus, Amazonas, Brazil. Malhi et al. (1998, 2002) and Araújo et al. (2002) describe these data in detail, so only a summary is presented here.

At the C14 site (2°35'S, 60°06'W), micro-meteorological data were collected from a 41.5 m tower situated on a broad plateau, with an eddy-covariance system mounted on a mast 5 m above the tower. At the K34 site (2°36'S, 60°12'W), located approximately 11 km southwest of the C14 site, meteorological data were collected from a 50 m tower situated on a medium sized plateau. Flux data were collected using an eddy-covariance system mounted on a mast 3 m above the tower. The forest canopy at both sites has a height of approximately 30 m and leaf area index (LAI) estimates for nearby sites range from 5.7 to 6.6 (Roberts et al., 1996).

The climate at these sites is characterised by little seasonal variation in temperature and solar radiation, and a large seasonal variation in rainfall. A short dry season from July to October occurs when the Intertropical Convergence Zone (ITCZ) is at its northern extreme. Total rainfall at C14 for the year 1 September 1995 to 31 August 1996 was 2088 mm, with 1118 mm falling during the study period of 1 September 1995 to 8 May 1996. This rainfall was close to the long-term average for Manaus city. The mean annual air temperature was 25.1 °C, with monthly means ranging from 24.2 °C in February to 26.9 °C in September. At K34, total rainfall for the year 16 June 1999 to 15 June 2000 was 2804 mm, making it one of the wettest years compared with the Manaus record. This rainfall anomaly has been linked with “La Niña” conditions in the equatorial Pacific (Araújo et al., 2002). Mean annual air temperature was 25.6 °C, with monthly means ranging from 24.4 °C in April to 26.8 °C in November.

The C14 flux data covered a period of just over seven months from 1 September 1995 to 8 May 1996, during which time most surface climate variables were available for all hours. Short periods of missing rainfall data were filled with data from a nearby forest site. For the seven month period, eddy-covariance water vapour, heat and CO₂ flux data were available for 53%, 63% and 53% of the time respectively. The K34 flux data covered a period of 11 months from 21 June 1999 to 23 May 2000. During this period, eddy-covariance water vapour, heat and CO₂ flux data were available for 75%, 76% and 75% of the time respectively.

The flux data at C14 had been reanalysed to include the effect of low frequency transport on

the observed fluxes (Malhi et al., 2002), which increased energy closure at this site from 77% to 94%. This equated to increases in mean water vapour, heat and CO₂ fluxes of 32.1%, 43.3% and 30.7% respectively. Energy closure at K34 was 76%, a value typical for eddy-covariance measurements at tropical forest sites. The raw data from K34 were not available, so the effect of the reanalysis procedure on closure at this site could not be included. Reanalysis of the raw data by Malhi et al. (2002) increased mean evaporation at C14 from 2.1 to 2.8 mm day⁻¹, still less than observations from other forest sites of 3.6 mm day⁻¹ (Shuttleworth, 1988; von Randow et al., 2004) and 3.9 mm day⁻¹ (Sommer et al., 2002). However, Malhi et al. and Harris et al. (2004) suggest that stomatal conductance between September and November 1995 at C14 was limited by low soil moisture, which may also have led to this relatively low evaporation rate.

If the mean flux increases from the C14 reanalysis were applied to K34, energy closure would increase to 102% and mean evaporation increase from 2.9 mm day⁻¹ to 3.8 mm day⁻¹, a value consistent with other estimates over Amazon rainforest. This correction to K34 was not applied in this study because of potential differences between the two sites. Using data taken concurrently at sites C14 and K34 during 1999–2000, Araújo et al. (2002) noted that maximum daytime CO₂ uptake was systematically higher at C14 than at K34. Their analysis suggested that this discrepancy was due to physical differences between the two sites and not measurement errors. Also, in this issue von Randow et al. (2004) applied the reanalysis procedure to the raw eddy-covariance data from a rainforest site in Southern Amazonia and only increased closure from 73% to 84%.

It is likely that the low evaporation rate seen at K34 was primarily due to poor energy closure, and the low evaporation rate seen at C14 was primarily due to soil moisture limitation. The reanalysed C14 data were used for the model calibration in this study because of the superior energy closure over K34, despite K34 having a longer and more complete dataset. As MOSES was calibrated against CO₂ fluxes, potential site differences should be kept in mind when comparing the performance of the calibrated model at site K34. However, they are also useful for assess-

ing which aspects of the calibration might be transferable between Amazonian rainforest sites.

Flux measurements from both sites indicate that the forest ecosystem is an unrealistically strong net carbon sink (Malhi and Grace, 2000). Possible reasons for this are that the eddy-covariance method systematically underestimates respiration during a stable nocturnal boundary layer, or that at night respired CO₂ is advected within the canopy and released in more open areas, such as river valleys. In either case, daytime fluxes are thought to be more reliable than night-time fluxes, so only CO₂ fluxes between 0800 and 1800 hours were used for model calibration.

The soils in this area are a yellow clay latosol (Brazilian classification) or oxisol (U.S. classification), with clay and sand content of 80% and 10% respectively. Hodnett et al. (1996b) calculate the available water capacity to be only about 70 mm m⁻¹ in the upper metre and about 30 mm m⁻¹ below 2 m. They estimate that the maximum water uptake below 2 m by vegetation can reach 250 mm in a dry year.

3. Model and methods

The land-surface model used in this study, MOSES, is currently used in Version 3 of the Hadley Centre GCM (HadCM3). A summary of elements relevant to this work follows; for a more comprehensive description the reader is referred to Cox et al. (1999) and Essery et al. (2001). MOSES calculates the surface energy, moisture and momentum balance for nine surface types (five vegetation and four non-vegetation) under the same near-surface forcing. The energy balance is calculated for each surface type separately as,

$$R_n = \lambda E + H + G \quad (1)$$

where R_n is net radiation at the surface (W m⁻²), λE is latent heat flux (W m⁻²), H is sensible heat flux (W m⁻²), and G is ground heat flux (W m⁻²). Net radiant energy is partitioned between latent, sensible and ground heat fluxes following a Penman-Monteith approach (see Monteith, 1965).

For vegetation surfaces, the canopy-level surface carbon balance is calculated as,

$$NEE = R_s - NPP \quad (2)$$

$$NPP = GPP - R_v \quad (3)$$

where NEE is net ecosystem exchange, ($\text{kgC m}^{-2} \text{s}^{-1}$), R_s is heterotrophic (soil) respiration ($\text{kgC m}^{-2} \text{s}^{-1}$), R_p is autotrophic (plant) respiration ($\text{kgC m}^{-2} \text{s}^{-1}$), NPP is net primary productivity ($\text{kgC m}^{-2} \text{s}^{-1}$) and GPP is gross primary productivity ($\text{kgC m}^{-2} \text{s}^{-1}$). Negative NEE values correspond to net carbon uptake by the land-surface.

Leaf-level net photosynthesis, A ($\text{mol CO}_2 \text{m}^{-2} \text{s}^{-1}$), is related to leaf-level stomatal conductance for water vapour, g_l (m s^{-1}), as a function of humidity deficit, D_* (kg kg^{-1}), leaf-surface temperature, T_* (K), and leaf-surface and internal CO_2 partial pressures, respectively c_c and c_i (both Pa) by the equation,

$$A = \frac{g_l}{1.6RT_*} (c_c - c_i), \quad (4)$$

where R is the gas constant, and the factor 1.6 accounts for g_l being conductance for water vapour rather than CO_2 . Potential (non-moisture stressed) leaf-level photosynthesis, A_p ($\text{mol CO}_2 \text{m}^{-2} \text{s}^{-1}$), is calculated using physiologically-based relationships for C_3 and C_4 plants (Collatz et al., 1991, 1992) and is related to A by

$$A = \beta A_p(\underline{X}, c_i), \quad (5)$$

where \underline{X} is a general vector of environmental variables, and β is the soil moisture availability factor. Photosynthetically active radiation (PAR) is taken to be a fraction 0.5 of incident solar radiation. The total soil moisture limitation factor, β , is calculated as a mean of β on each soil level, β_r , weighted by a depth-dependent root density, such that

$$\beta_r = \begin{cases} 0 & \theta_r \leq \theta_w \\ \frac{\theta_r - \theta_w}{\theta_c - \theta_w} & \theta_w < \theta_r < \theta_c \\ 1 & \theta_r \geq \theta_c \end{cases} \quad (6)$$

where θ_r is soil moisture content of a soil layer ($\text{m}^3 \text{m}^{-3}$), and θ_c and θ_w are the critical and wilting soil moisture contents respectively (both $\text{m}^3 \text{m}^{-3}$). Equations (4) and (5) contain three unknowns, A , g_l and c_i , for which closure is obtained following the method of Jacobs (1994):

$$\left(\frac{c_i - \Gamma}{c_c - \Gamma} \right) = f_0 \left(1 - \frac{D_*}{D_c} \right) \quad (7)$$

where Γ (mol m^{-3}) is the CO_2 photorespiration compensation point, and f_0 and D_c (kg kg^{-1}) are fitting parameters.

Scaling conductance and photosynthesis from leaf- to canopy-level is done following the method of Sellers et al. (1992), by which top-of-canopy leaf-level values are multiplied by a function of leaf area index, L , to yield canopy-level values:

$$f_{\text{par}} = \frac{1 - e^{-0.5 L}}{0.5}. \quad (8)$$

GPP and R_p in Eq. (3) are calculated as functions of canopy-scale photosynthesis, A_c .

In standard GCM configuration, MOSES has four soil layers extending to a total depth of 3 m. There are three soil types (fine, medium and coarse) with thermodynamic and hydrological parameters defined in look-up tables. Root depth is 3 m for broadleaf trees, and root density decreases exponentially with depth. Soil matric potential, ψ (kPa), hydraulic conductivity, k (mm h^{-1}), and soil moisture content, θ , are related following Campbell (1974) using Eqs. (9) to (11).

$$S = \frac{\theta}{\theta_s} \quad (9)$$

$$\psi = \psi_s (S)^{-b} \quad (10)$$

$$k = k_s (S)^{2b+3} \quad (11)$$

where ψ_s , k_s and θ_s are the matric potential, hydraulic conductivity and soil moisture volume fraction respectively at saturation, and S is the non-dimensional relative saturation. Transpiration is unlimited by soil moisture for ψ greater than -33 kPa ($\beta = 1$), but below that point limitation increases linearly with θ until transpiration ceases for ψ less than -1500 kPa ($\beta = 0$).

Table 1 gives values for site-specific parameters that were fixed in all simulations. Only the broadleaf tree surface type was used because

Table 1. Site-specific parameters used in all MOSES simulations at each site. Zero plane displacement was calculated as 0.86 h following Shuttleworth (1989). Reference height was defined as the vertical distance between zero plane displacement and the height at which observations were taken

Parameter	C14 site	K34 site
Soil carbon, C_s (kg m^{-2})	6.24	6.24
Canopy height, h (m)	30.0	30.0
Zero plane displacement, z_0 (m)	25.8	25.8
Reference height, z_r (m)	20.7	24.2
Leaf area index, LAI	5.5	5.5

the forest was continuous to distances greater than the fetch of the instruments. The performance of MOSES in standard setup is assessed for both C14 and K34 sites. Parameters for calibration are identified, and calibrated against re-analysed C14 data by minimising normalised root mean squared errors in NEE and λE fluxes. The resulting calibration is then tested against independent flux data from K34.

4. Results

4.1 Uncalibrated MOSES

Mean observed and modelled fluxes of heat, moisture and carbon are shown in Table 2 for the C14 and K34 sites. Results are quoted as mean per day values to allow comparison of the two sites. Observed mean evaporation through the study periods was similar for both sites at 2.8 mm day^{-1} for C14 and 2.9 mm day^{-1} for K34. Uncalibrated MOSES was in good agreement with observations at both sites with mean evaporation rates of 2.9 mm day^{-1} and 3.2 mm day^{-1} at C14 and K34 respectively. Observed mean heat fluxes through the study periods (in units of equivalent moisture flux) differed between the sites with 1.3 mm day^{-1} at C14 and 0.8 mm day^{-1} at K34. Uncalibrated MOSES simulated a similar mean heat flux for both sites of 1.6 mm day^{-1} , which corresponded to a greater overestimation for K34 than for C14. The observed Bowen ratio ($\lambda E/H$) for C14 was somewhat high at 0.46, while the K34 ratio of 0.28 was more typical of rainforest sites. The modelled Bowen ratios were similarly high for both sites with 0.55 and 0.50 for C14 and K34 respectively. Malhi et al. (2002) and Harris et al. (2004) suggest that low soil moisture content at C14

through the first few months of the study period (September–November 1995) limited evaporation at this site, which may explain partly the high Bowen ratio there. Conversely, K34 evaporation was not limited by soil moisture and exhibited a more usual Bowen ratio. The reanalysis procedure included in the C14 data tends to preserve the Bowen ratio while increasing the magnitude of latent and sensible heat fluxes to improve energy closure. So, it is likely that the discrepancy between modelled and observed Bowen ratios at K34 were a deficiency of the model rather than an artifact of imperfect energy closure.

Mean observed daytime NEE flux was $-150 \text{ kgC ha}^{-1} \text{ day}^{-1}$ at C14 and $-107 \text{ kgC ha}^{-1} \text{ day}^{-1}$ at K34. As explained in Section 2, nighttime carbon fluxes were considered to be unreliable, so only observations between the hours of 0800 and 1800 local time were included in these means. For this reason the NEE totals and mean flux rates quoted here should not be regarded as true net carbon balances of the sites. Over daytime hours, uncalibrated MOSES underestimated the mean NEE flux as $-56.8 \text{ kgC ha}^{-1} \text{ day}^{-1}$ at C14 and $-47.8 \text{ kgC ha}^{-1} \text{ day}^{-1}$ at K34.

Figure 1 shows ten day mean observed and modelled fluxes of moisture, heat and carbon for both sites. At C14, MOSES in default setup tended to overpredict evaporation at the beginning of the study period (October, November) and underpredict in the following months (December, January). At both sites the model exhibited less variability in evaporation through the study period than was seen in the observations. For heat flux, Fig. 1c shows that the model performed well through most of the study period at C14, but began to overestimate during March and April, the last two months of the run. At K34, however,

Table 2. Mean observed and modelled fluxes of moisture, E (mm day^{-1}), heat, H (mm day^{-1}), and carbon, NEE ($\text{kg C ha}^{-1} \text{ day}^{-1}$), at sites C14 and K34. Heat fluxes are shown in units of equivalent evaporation. Also given are the number of observations, n , over which the means were taken. For NEE, only observations between the hours of 0800 to 1800 inclusive were used. Observations for C14 include the reanalysis of Malhi et al. (2002)

	C14 site			K34 site		
	E	H	NEE	E	H	NEE
Observed	2.8	1.3	-150	2.9	0.8	-107
Default	2.9	1.6	-56.8	3.2	1.6	-47.8
STOM	3.4	1.1	-128	4.0	0.5	-128
SOIL	2.9	1.5	-98.1	3.7	0.9	-117
n	3094	3648	1155	12942	13211	4879

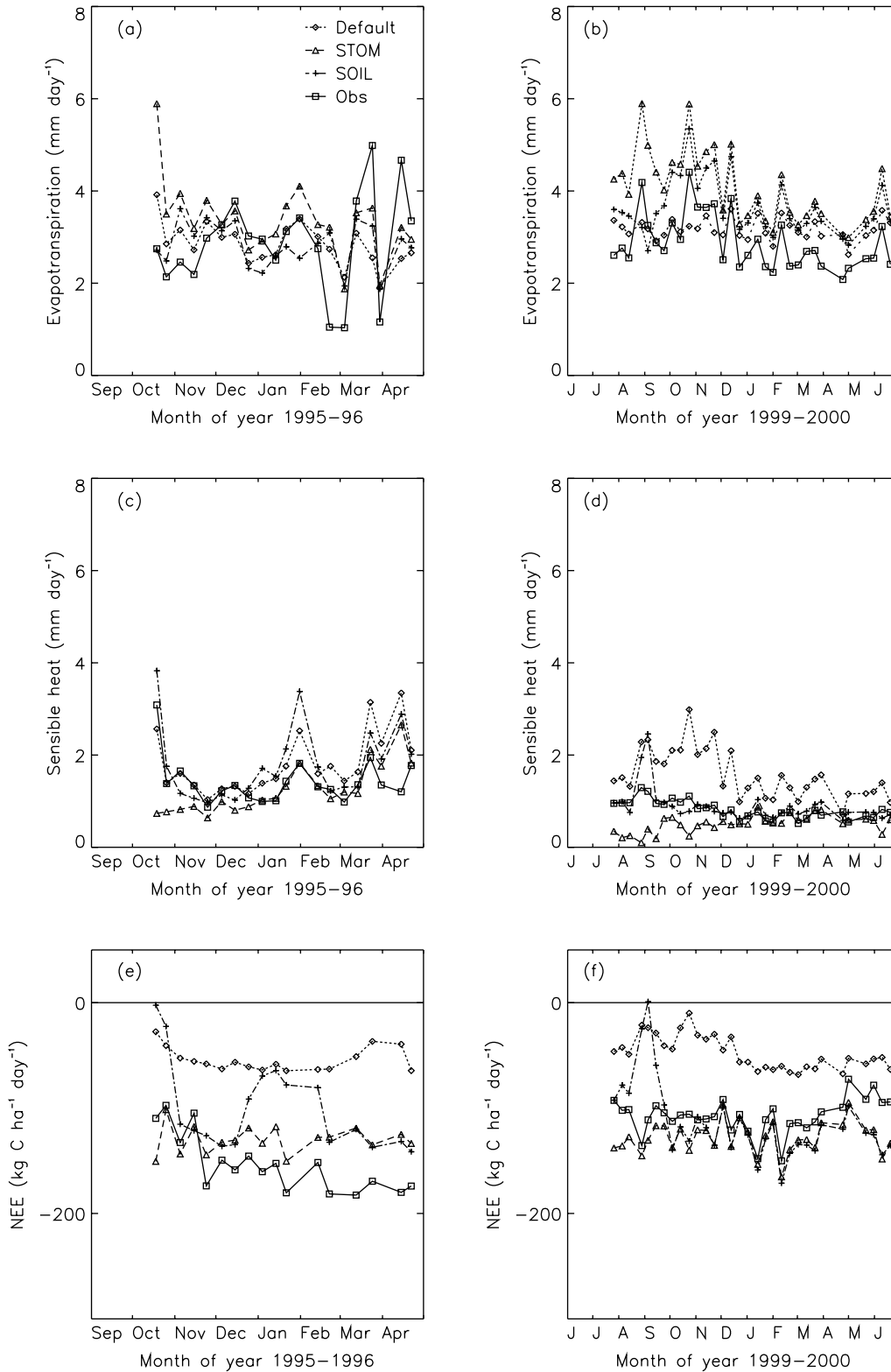


Fig. 1. Observed and modelled 10 day mean (a, b) evapotranspiration, (c, d) sensible heat flux, and (e, f) net ecosystem exchange for the C14 and K34 tower sites respectively. Sensible heat fluxes are shown in units of equivalent moisture flux (mm). For NEE, only data between the hours of 0800 and 1800 inclusive were included

the model overestimated heat flux all through the study period (Fig. 1d). Figure 1e and 1f show that the NEE underestimation occurred throughout both of the model runs and was not restricted to any particular period or time of year.

Mean diurnal cycles of moisture, heat and carbon fluxes for dry months (July to December) and wet months (January to June) are shown in

Fig. 2 for C14 and Fig. 3 for K34. In addition to the seasonal errors identified from the ten day means, there was a tendency for modelled evaporation and NEE to decline after 1000 h rather than continuing to rise to a diurnal maximum at 1200 h, as observed. At the same time, sensible heat fluxes became greater than observed, especially at K34, suggesting an incorrect stomatal

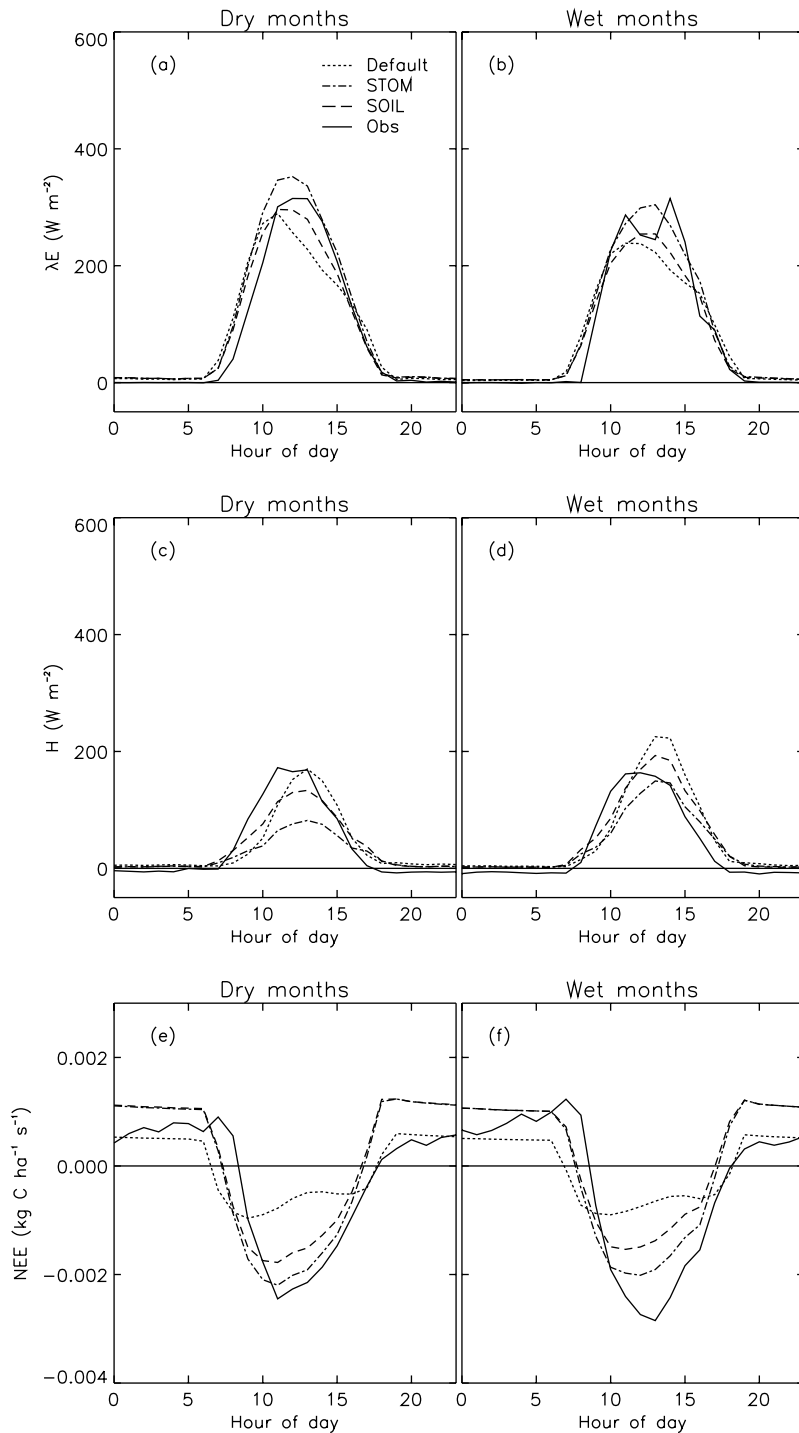


Fig. 2. Mean modelled and observed diurnal cycles of (a, b) latent heat flux, (c, d) sensible heat flux and (e, f) net ecosystem exchange for dry months (October–December 1995) and wet months (January–April 1996) at the C14 tower site

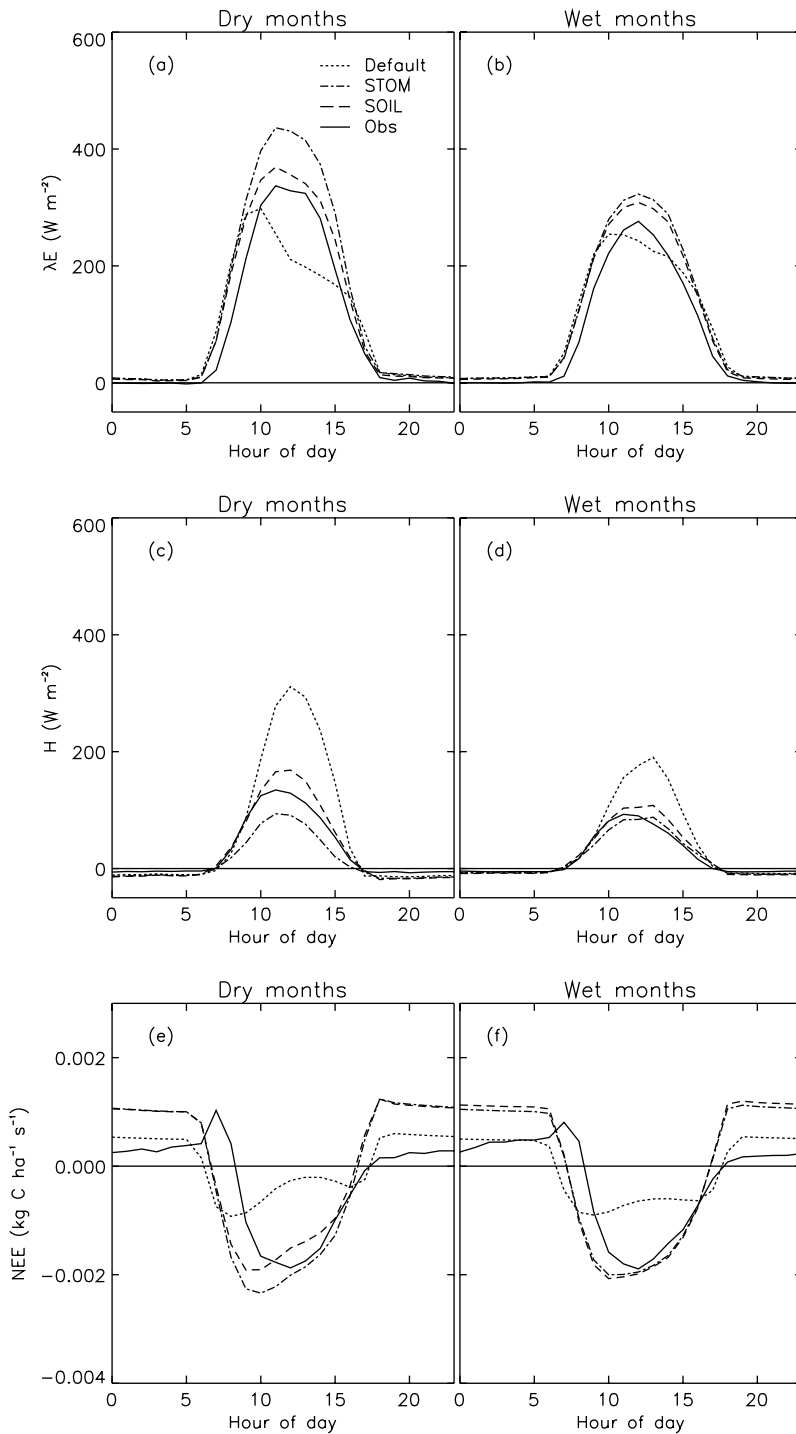


Fig. 3. Mean modelled and observed diurnal cycles of (a, b) latent heat flux, (c, d) sensible heat flux and (e, f) net ecosystem exchange for dry months (July–December 1999) and wet months (January–May 2000) at the K34 tower site

response to environmental conditions. There was also a persistent phase difference between modelled and observed heat flux at C14 such that the model lagged observations by 1–2 hours. This was due to modelled ground heat fluxes of $\pm 60 W m^{-2}$ during morning and afternoon.

Estimates of canopy (or bulk-stomatal) conductance, g_c , were calculated from moisture flux data

using an inverted Penman-Monteith equation (Monteith, 1965). To avoid periods of wet-canopy evaporation g_c estimates were filtered to exclude the 24 hours following any rainfall event. Mean dry and wet month diurnal cycles of observed and modelled g_c for both sites are shown in Fig. 4. Stomatal closure from mid-morning to mid-afternoon caused a persistent underprediction

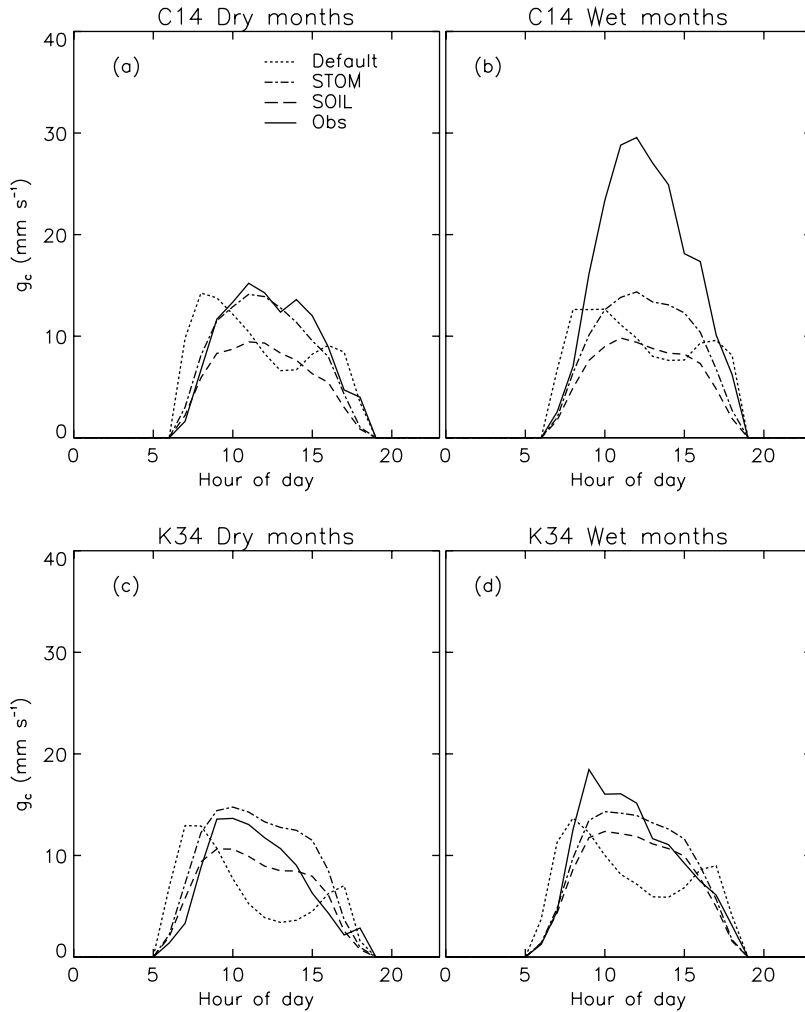


Fig. 4. Mean diurnal cycles of canopy conductance for (a, b) C14 and (c, d) K34 tower sites. The respective observations periods and definition of dry and wet months are given in the captions to Figs. 2 and 3. Calculated from eddy-correlation measurements of evaporation and an inverted Penman-Monteith equation. Observations and model values are filtered to include only the hours 0600 to 1800, and to exclude the 24 hours after any rainfall to avoid periods when wet-canopy evaporation rather than transpiration dominates

of daytime maximum g_c by MOSES. This problem was reflected most severely in modelled NEE where the diurnal maximum was only about 50% of that observed.

The photosynthesis sub-model was isolated to estimate the potential maximum rate of carbon uptake in the model. A soil carbon content of 6.24 kgC m^{-2} and mean soil temperature of 27°C were assumed, which gave a soil respiration of $0.4 \times 10^{-3} \text{ kgC ha}^{-1} \text{ s}^{-1}$. In optimal environmental conditions, the maximum possible simulated NEE was approximately $-1 \times 10^{-3} \text{ kgC ha}^{-1} \text{ s}^{-1}$. Maximum observed NEE values during the wet season were approximately $-3 \times 10^{-3} \text{ kgC ha}^{-1} \text{ s}^{-1}$ at C14 and $-2 \times 10^{-3} \text{ kgC ha}^{-1} \text{ s}^{-1}$ at K34. So, even in conditions of high light levels, low humidity deficit and saturated soil moisture, when stomata would be at their most open, it was not possible for modelled NEE to match observed daily maximum values.

Figure 4 also shows that MOSES did not exhibit differences in daily maximum g_c between wet and dry months seen in the observations at C14 and to a lesser extent at K34. Harris et al. (2004) and Malhi et al. (2002) attribute the seasonal variation at C14 to changes in soil moisture content rather than changes in solar radiation, temperature or humidity. MOSES did not simulate moisture stress at either site using either the default or STOM parameters, which suggested the default soil parameters were inappropriate for this region. These two problems occur on different time scales (diurnal and seasonal) and so were amenable to investigation and calibration separately.

4.2 Calibrated stomatal model

From the results of Section 4.1, two parameters in the Jacobs closure equation (Eq. (7)) and two

parameters in the photosynthesis submodel were identified for calibration. These were, D_c , critical humidity deficit (kg kg^{-1}); f_0 , ratio of leaf-internal to leaf-surface CO_2 partial pressures at saturation; N_{l0} , top leaf nitrogen-carbon ratio (kg(N) kgC^{-1}); α , quantum efficiency ($\text{mol(CO}_2\text{) mol(PAR)}^{-1}$). The modelled stomatal response (i.e. canopy conductance, g_c) is affected primarily by f_0 and D_c through temperature and humidity deficit, and by N_{l0} and α through the rate of photosynthesis.

The model was calibrated by minimising the objective function,

$$F = \frac{\sum_{i=1}^{n_1} (E_{im} - E_{io})^2}{\sum_{i=1}^{n_1} (E_{io} - \bar{E}_o)^2} + \frac{\sum_{j=1}^{n_2} (NEE_{jm} - NEE_{jo})^2}{\sum_{j=1}^{n_2} (NEE_{jo} - \overline{NEE}_o)^2}$$

against observed flux data from the C14 site including reanalysis by Malhi et al. (2002), where E (mm s^{-1}) is the rate of evaporation from the surface. A constant value for the latent heat of vaporisation, λ , of 2.501 MJ kg^{-1} when converting between evaporation rate and latent heat flux. The subscript ‘o’ refers to observations, ‘m’ to modelled values, and n_1 and n_2 are the number of observations of E and NEE respectively. Observed profiles of canopy CO_2 were not available for calculating CO_2 storage within the canopy airspace, which can account for a significant discrepancy between NEE in the morning. It was assumed that the effect of neglecting canopy storage was minimised by only using data between 0800 and 1800 hours. Ideally the model would have been calibrated against observed NPP rather than NEE , but observations of soil respiration were not available, and it was considered inappropriate to use uncertain estimates from empirical functions of soil temperature. Araújo et al. (2002) recently observed a mean soil respiration efflux in Reserva Cuieiras forest of $67 \text{ kgC ha}^{-1} \text{ day}^{-1}$ with only a small diurnal range, whereas daytime NEE regularly peaks at around $-260 \text{ kgC ha}^{-1} \text{ day}^{-1}$ with a much larger diurnal range than soil respiration. Because of this it was assumed that the daytime stomatal response could be calibrated from NEE without too much interference from the diurnal cycle of soil

Table 3. Parameters used in the stomatal conductance and photosynthesis components of MOSES. Default values refer to the ‘broadleaf tree’ plant functional type defined in MOSES. STOM is the calibrated parameters when the medium soil type is used. SOIL is the calibrated parameters when the soil parameters given in Tables 4 and 5 are used

	f_0	D_c (kg kg^{-1})	N_{l0} (kg(N) kg(C)^{-1})	α ($\text{mol(CO}_2\text{) mol(PAR)}^{-1}$)
Default	0.875	0.090	0.040	0.080
STOM	0.650	0.182	0.174	0.057
SOIL	0.685	0.185	0.207	0.066

respiration. Sensible heat flux measurements were not used in the objective function as the phase difference between model and observations led to large hourly errors which strongly biased the optimisation.

The resulting optimised parameters when a medium soil type was used (STOM) are given in Table 3 along with the MOSES default values for broadleaf trees. When the STOM parameters were used the modelled mean evaporation at C14 increased to 3.4 mm day^{-1} and mean sensible heat flux decreased to 1.1 mm day^{-1} . Mean NEE decreased to $-128 \text{ kgC ha}^{-1} \text{ day}^{-1}$. Ten day mean values of NEE (Fig. 1c) show that NEE decreased for all months of the study period to be in better agreement with observations.

Results were similar when the STOM parameters calibrated at C14 were used to simulate the K34 data. Mean evaporation increased to 4.0 mm day^{-1} and mean sensible heat flux decreased to 0.5 mm day^{-1} . The changes in mean latent and sensible heat flux at each site corresponded to reduced Bowen ratios of 0.32 and 0.13 at C14 and K34 respectively. These values were lower than observed and indicate that improving the modelled carbon uptake degraded the modelled energy partition at both sites. Figure 1b and 1d show that much of the discrepancy in the mean was from errors in the dry season between July and December 1999. During the wetter succeeding months, modelled heat and moisture fluxes agreed well with observations. Furthermore the modelled variability between months was in better agreement with observations than when the default parameters were used. NEE decreased throughout the run to be in good agreement with observations, with mean

NEE decreasing to $-128 \text{ kgC ha}^{-1} \text{ day}^{-1}$, the same rate of carbon uptake modelled for C14 using the STOM parameters.

Mean dry and wet month diurnal cycles of λE , H and NEE using the STOM parameters are shown in Figs. 2 and 3. Calibration limited the afternoon decline in λE and NEE seen in the default model, and allowed NEE to achieve a more realistic daytime maximum. This is reflected in an improved simulation of the diurnal cycles of g_c at both sites (Fig. 4). However, the calibrated model exhibited little of the seasonal variation in daytime maximum g_c seen in observations. This was most obvious at C14 where the model overestimated g_c through the end of the dry season and underestimated g_c through the beginning of the wet season (Fig. 4). Observations indicate that during the study period g_c was limited by soil moisture. Modelled soil moisture was lower than observed in both runs (Fig. 5b), but the soil moisture limitation factor, β , remained equal to unity for most of the run period (Fig. 6). This resulted in both the default

and calibrated models exhibiting little of the observed variation in g_c between months.

4.3 Soil parameters

Correa (1984) and Hodnett et al. (1996b) estimate that soils in the region of these tower sites have a plant available water content of about 130 mm over the top 3 m, and 30 mm m^{-1} below this. In contrast, the default soil type used in HadCM3 for this region has a plant available water content of 966 mm over the top 3 m, with roughly 648 mm extractable before stomatal conductance is limited by soil moisture. This means that MOSES is able to satisfy demand for water with extraction from the top 3 m of soil without moisture limitation. It should be noted that the soil parameters used in a GCM are chosen to represent the functioning of a large area, typically $\sim 10^4 \text{ km}^2$, so should not be expected to represent accurately individual sites within that area. Measurements in this area indicate that during most years the forest has to extract water

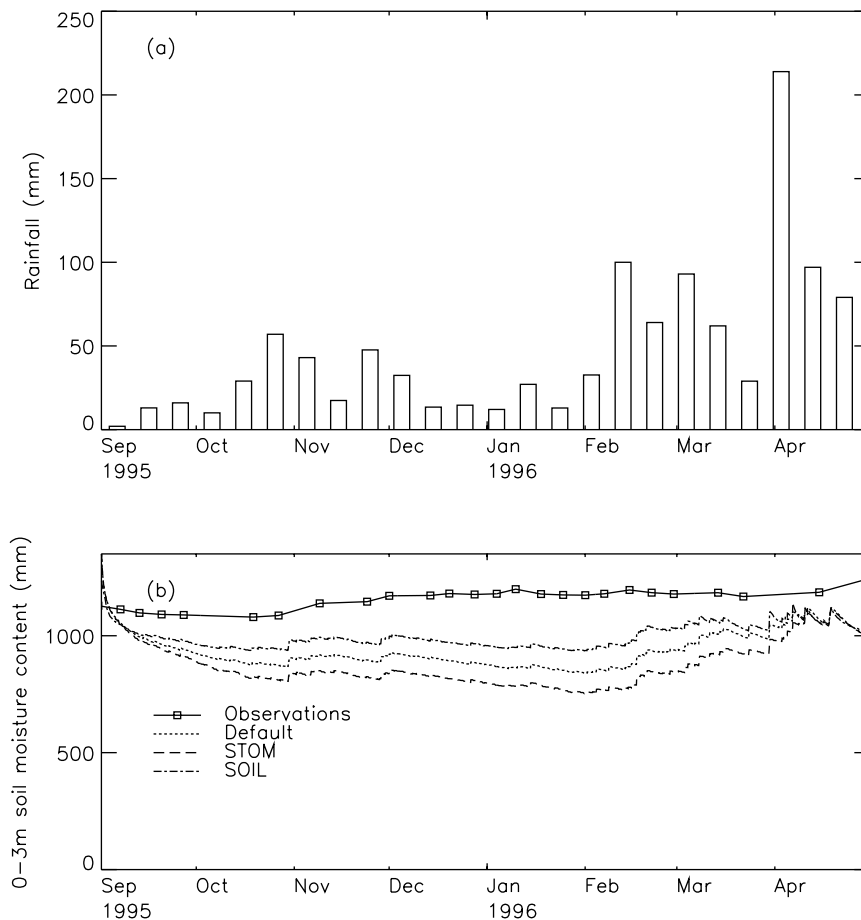


Fig. 5. Observed values of (a) 10 day totals of rainfall (b) total soil moisture content in the top three metres for the C14 tower site. Also shown in (b) are the modelled total soil moisture content in the top three metres

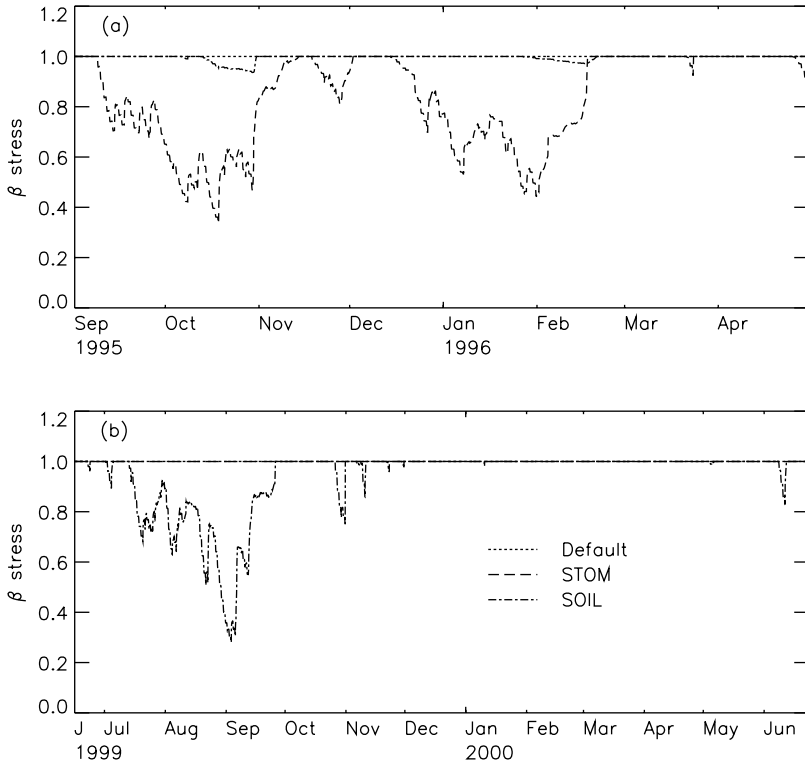


Fig. 6. Modelled soil moisture stress function, β , for (a) C14 and (b) K34 sites. When $\beta = 1$ the vegetation is experiencing no stress due to soil moisture deficit, and stomatal conductance is limited only by temperature, humidity, light and CO_2 . When $\beta = 0$ stomata are completely closed in response to low soil moisture content, so transpiration and photosynthesis cease

from depths between 2 m and 9 m (Hodnett et al., 1996b). Roots have been found as deep as 12 m in Amazonian rainforest (Nepstad et al., 1994), but it is unclear to what extent they are used for water extraction. Root depth was kept at 3 m because of uncertainties in the way forests use deep roots for water uptake and because soil parameters were not available for greater depths.

New depth-dependent soil parameters for MOSES were generated from soil parameters measured at a nearby forest site with similar textural properties (Wright et al., 1996). The parameters taken from Wright et al. were those for a van Genuchten (1980) (VG) scheme ($\alpha_{\text{soil}}, n, \theta_s, \theta_r, k_s$) rather than for the Campbell (1974) scheme (ψ_s, b, θ_s, k_s) used in MOSES. Algebraic relations, such as those in Lenard et al. (1989) and Morel-Seytoux et al. (1996), allow the VG parameters α_{soil} and n to be converted to the equivalent Campbell parameters, ψ_s and b in Eqs. (10) and (11). However, the two schemes still differ in their definition of relative saturation, Eq. (9). The VG scheme includes a residual soil moisture content such that when S equals zero, there is θ_r unextractable moisture left in the soil, whereas the Campbell scheme assumes that all moisture can be extracted. In

many soils θ_r is close to zero or very low compared to θ_s , in which case there is little difference between the VG definition of relative saturation and Eq. (9). However, for the clay soils in this region, θ_r is a significant fraction of θ_s , so could not be neglected. This difference was easily accounted for, by redefining θ in Eq. (9) as,

$$\Theta = \theta - \theta_r, \quad (12)$$

and adjusting dry soil heat capacity, C_{dry} , and dry soil heat conductivity, λ_{dry} , to account for the thermal properties of the residual moisture at $\Theta = 0$.

Depth dependent Campbell parameters, converted from VG parameters using the relation of Lenard et al. (1989), are shown in Tables 4 and 5. Lower saturated and wilting points meant that plant available water content in the top 3 m was reduced from 966 mm to 327 mm. Residual moisture content was $0.3 \text{ m}^3 \text{ m}^{-3}$ at each level. Lower values for the exponent, b , meant that k and ψ were more sensitive to changes in soil moisture content. With these new soil parameters, f_0, D_c, N_{l0} and α were again optimised using the same method as in Section 4.2, and the resulting parameter set (SOIL) is shown in Table 3.

Table 4. Soil parameters used in MOSES runs. Default refers to the parameters used in HadCM3 for the grid box containing the field sites studied herein. In this case the parameters do not vary with depth. The depths correspond to a depth dependent set of parameters calculated using the equivalence relation of Lenard et al. (1989) to convert van Genuchten parameters from a nearby site. A residual moisture content of $0.3 \text{ m}^3 \text{ m}^{-3}$ was assumed at each depth

	b	ψ_s (m)	θ_s ($\text{m}^3 \text{ m}^{-3}$)	θ_c ($\text{m}^3 \text{ m}^{-3}$)	θ_w ($\text{m}^3 \text{ m}^{-3}$)	C_{dry} ($\text{MJ K}^{-1} \text{ m}^{-3}$)
Default	6.60	-0.049	0.458	0.242	0.136	1.19
5 cm	2.60	-0.105	0.210	0.055	0.013	2.30
22.5 cm	2.40	-0.093	0.130	0.029	0.006	2.62
67.5 cm	2.85	-0.030	0.130	0.025	0.007	2.69
200 cm	1.50	-0.370	0.100	0.023	0.002	3.12

Table 5. Caption as per Table 4. Thermal and hydraulic conductances in MOSES are defined at the boundaries of soil levels rather than the mid-point

	k_s (mm h^{-1})	λ_{dry} ($\text{W m}^{-1} \text{ K}^{-1}$)
Default	16.92	0.230
0 cm	399.6	0.446
10 cm	421.2	0.536
35 cm	590.4	0.564
100 cm	568.8	0.655
300 cm	5.004	0.689

The stomatal parameter set SOIL was similar to STOM, indicating that improvements made to the diurnal stomatal response were not affected by the change in soil parameters. In the SOIL simulation mean evaporation at C14 was 2.9 mm day^{-1} and mean heat flux was 1.5 mm day^{-1} , similar to observations and default MOSES. At K34, mean evaporation was overestimated at 3.7 mm day^{-1} , but mean heat flux was similar to observations at 0.9 mm day^{-1} . Modelled Bowen ratios were 0.51 at C14 and 0.24 at K34, which was an agreement with observed values at both sites not seen in simulations with either the default or STOM parameters. Figures 2a, c and 3a, c show that at K34 this was mainly due to an improved simulation of the energy partition in dry months, during which time soil moisture stress was simulated at both sites (Fig. 6), even though during the K34 study period there was above average rainfall. At C14 the reduced dry month g_c required to gain this improvement degraded the model relative to observations (Fig. 4a), and the model was still unable to simulate midday g_c values of 30 mm s^{-1} in wet months.

Mean NEE was $-98.1 \text{ kgC ha}^{-1} \text{ day}^{-1}$ at C14 and $-117 \text{ kgC ha}^{-1} \text{ day}^{-1}$ at K34, which at both sites corresponded to a decrease in the rate of net carbon uptake relative to the STOM simulations. Only at C14 did this also mean modelled NEE worsened relative to the observed value, and this was due to a combination of low canopy conductance through the whole simulation and a period of soil moisture stress between December and February. Unlike during October 1995, the model was able to maintain latent heat flux through this period of soil moisture stress by wet-canopy evaporation.

5. Discussion

The results presented here show that there is potential for improving GCM land-surface model simulation of surface fluxes over Amazonian rainforest. When a closed carbon cycle has been included in climate models it has shown that perturbations to the carbon cycle could have a significant impact on climate through this next century, with particular implications in Amazonia (Cox et al., 2000, 2004). Furthermore, much of the regional climate change over Amazonia can be attributed to the response of the modelled land-surface (Betts et al., 2004). It is, therefore, important that attention is given to the simulation of CO_2 flux as well as heat and moisture fluxes.

Historically, emphasis has been placed on improving the simulation of heat and moisture fluxes due to their importance in the hydrological cycle simulated by climate and operational forecast models. So it is unsurprising that uncalibrated MOSES simulated these fluxes more successfully than CO_2 flux. The fact that calibrating MOSES against C14 NEE and latent heat

fluxes improved the mean daytime carbon uptake but degraded the mean evaporation highlights the problem of calibrating SVATs against multiple simultaneous observations. Bastidas et al. (1999) demonstrate that parameter sets that are optimal for the simulation of one variable may not be optimal for simulating a second, due to model imperfections. This is especially the case when the observations are not physically constrained by a joint conservation law (e.g. for mass or energy), where improving the simulation of one would necessarily improve the simulation of the other. While the simulated mean evaporation at C14 agreed with observations, this masked a tendency to overpredict in the morning between 0600 and 1000 hours, and underpredict through the afternoon due to an incorrect stomatal response. Calibration greatly reduced the tendency for afternoon stomatal closure, thus improving the diurnal cycle of both λE and NEE.

As with many eddy-covariance data from forest sites, energy closure at K34 was poor, so care must be taken when comparing modelled and observed fluxes of latent and sensible heat for this site. The fact that the Bowen ratio is often preserved when data are reanalysed using a method such as Malhi et al. (2002) to improve closure makes it a useful diagnostic for comparing models against datasets with imperfect closure. Calibration of the stomatal response along with revised soil parameters improved the modelled Bowen ratios at both sites, but soil moisture stress was required to simulate the observed Bowen ratio at K34 even though there was above average rainfall. This reflects the modelling study of Williams et al. (1998), who found that without soil moisture constraints they were unable to simulate dry season carbon dioxide and water vapour fluxes over Amazonian rainforest. von Randow et al. (2004) observed that Bowen ratios calculated using eddy-covariance observations of λE are often greater than those where λE is calculated from the residual of energy balance. Observed Bowen ratios calculated using the residual of energy balance at C14 and K34 were 0.41 and 0.20 respectively. These values were lower than when eddy-covariance values of λE were used, but the reduction was not sufficient for the STOM simulation to agree more closely than the SOIL simulation with these observations. So the simulation of soil moisture stress at these

sites could not be explained by this uncertainty in the observed Bowen ratio.

Figure 7 shows the response of canopy level NEE in MOSES to surface meteorology with default and calibrated stomatal parameters. Soil respiration was calculated using a soil carbon content of 6.24 kg m^{-2} , a soil temperature equal to the air temperature (26°C in Fig. 7a–c and as per temperature axis in Fig. 7d) and no soil moisture stress. The difference between the STOM and SOIL calibrated parameters was relatively small, so the following points for the STOM parameters also apply to the SOIL parameters. Generally, the effect of the parameter changes was to decrease NEE in all meteorological conditions. The sensitivity of NEE to changes in air pressure (Fig. 7a) and humidity deficit (Fig. 7b) remained roughly the same after calibration. The shift in the humidity deficit curve meant that it had to reach a much higher level before NEE would reach zero, and so the modelled vegetation would have less of a tendency to conserve water during periods of high atmospheric demand. However, typical air humidity deficits in the forest range from 0 to 17 g kg^{-1} , so those extreme situations are not met in practice. The response to temperature is constrained in the model such that stomatal conductance is zero below 0°C and above 36°C . Upon calibration, the greatest decrease in NEE occurred for temperatures near the optimum value, while the optimal temperature itself decreased slightly from 27.1°C to 25.4°C , making the NEE response more symmetrical about the midpoint of 26°C . This optimum was roughly equal to the mean air temperature for these forest sites, which agrees with the idea that the optimal temperature is close to the mean annual growing season temperature (Sellers et al., 1997).

There was a noticeable difference in the calibrated response to solar radiation (Fig. 7c). With default MOSES, canopy-level photosynthesis saturated for incident solar radiation greater than about 200 W m^{-2} . However, in the calibrated model, NEE increased more gradually with radiation and did not begin to saturate until approximately 400 W m^{-2} . Other things being equal, this had the effect of increasing midday NEE and reducing NEE at the beginning and end of the day and through the night. Observa-

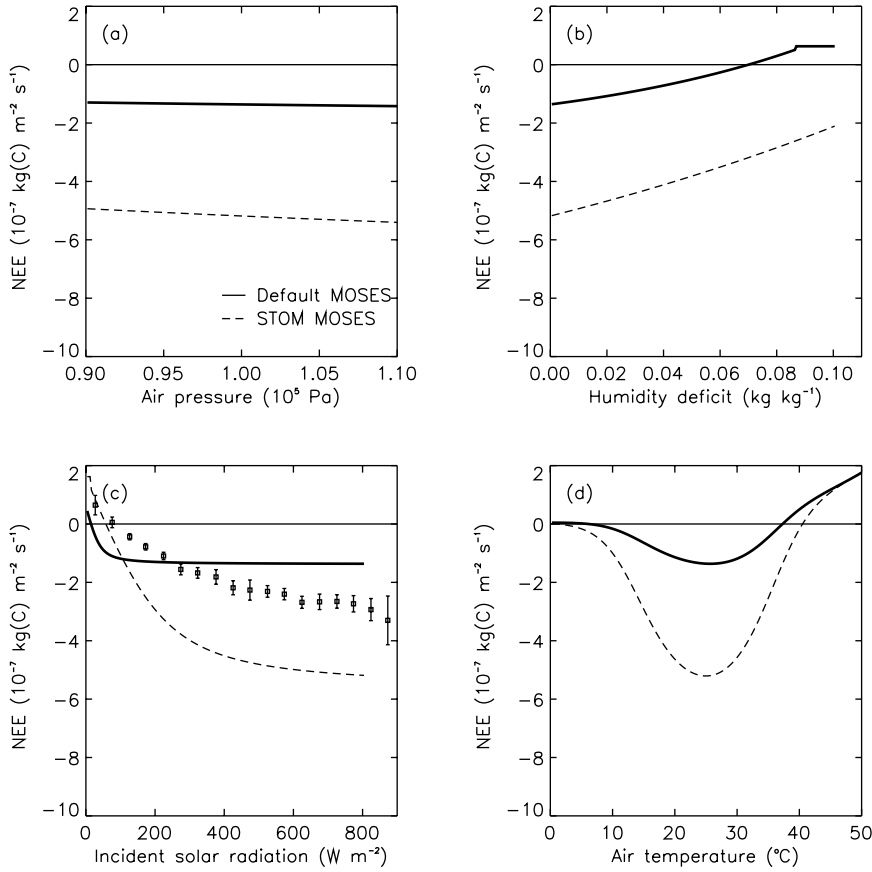


Fig. 7. Typical responses of canopy level NPP in MOSES to (a) air pressure, (b) humidity deficit, (c) incident solar radiation, and (d) air temperature before and after calibration. When one quantity was varied the others were set to constants: $p_* = 1000$ hPa, $D = 0.01$ g kg⁻¹, $S = 800$ W m⁻², $T = 26$ °C

tions from C14 (shown by means over 50 W m⁻² bins in Fig. 7c) reflect this lack of saturation in NEE at low solar insolation. Minimum observed NEE tends to a value approximately 2×10^{-7} kgC m⁻² s⁻¹ lower than the model value due to limitation by environmental factors other than solar radiation. von Randow et al. (2004) show a similar saturation response to solar radiation with NEE reaching -3×10^{-7} kgC m⁻² s⁻¹ above 430 W m⁻² (assuming that PAR is a factor 0.5 of incident solar radiation). Furthermore, von Randow et al. place the point of zero NEE at about 100 W m⁻², which agrees well with C14 data and the modelled value of 60 W m⁻².

The effect on NEE of the calibration can be broken down by individual parameters. The change in α from 0.080 to 0.057 mol(CO₂) mol(PAR)⁻¹ upon calibration brought it in closer agreement with observed values of 0.051 mol(CO₂) mol(PAR)⁻¹ (Fan et al., 1990) and 0.048 mol(CO₂) mol(PAR)⁻¹ Malhi et al. (1998), but led to negligible changes in NEE. The value of D_c was doubled, which had the effect of increasing the humidity deficit at

which NEE falls to zero, while leaving NEE at zero humidity deficit unchanged. The change in f_0 had the opposite effect of the D_c change in that it decreased NEE at zero humidity deficit and left the point at which NEE becomes zero unchanged. The combined effect of these two parameters alone was to make NEE less sensitive to changes in humidity deficit. However, the combined effect of calibrating f_0 , D_c and N_{l0} (neglecting α) was to maintain the same response to changes in humidity deficit, while increasing NEE through the response to temperature and solar radiation. The reduction in modelled canopy conductance around midday seen in Fig. 4 for the default model coincides with the diurnal cycle of humidity deficit which has a maximum around 1400 h. It is likely that this was the result of the humidity deficit response dominating in the presence of a saturated solar response. But the calibration suggests that the default humidity response was correct.

The optimised values of leaf nitrogen, N_{l0} , corresponded in MOSES to increases in the

maximum rate of carboxylation of rubisco, V_{\max} , from 32 to 139 $\mu\text{mol CO}_2 \text{ m}^{-2} \text{ s}^{-1}$ (STOM) and 166 $\mu\text{mol CO}_2 \text{ m}^{-2} \text{ s}^{-1}$ (SOIL). These values were higher than other optimised model values of V_{\max} of 81.8 $\mu\text{mol CO}_2 \text{ m}^{-2} \text{ s}^{-1}$ (da Rocha et al., 1996) and 79.4 $\mu\text{mol CO}_2 \text{ m}^{-2} \text{ s}^{-1}$ (Sen et al., 2000) reported for rainforest at Reserva Jaru, and as such are probably unrealistically high. The large change in N_{10} required to simulate the observed light response for this forest suggests an alternative model parameterisation may be necessary for MOSES to be consistent with both the observed light response and N_{10} .

It is possible that, through the response to solar radiation, the increase in N_{10} is compensating for the effect of self-shading or a canopy nitrogen profile that is not proportional to PAR (Friend, 2001). The big-leaf scaling from leaf-level to canopy-level photosynthesis assumes that the response of the whole canopy to light is the same as for leaves at the top of the canopy. However, for vegetation with a high LAI, leaves lower in the canopy are shaded and so receive diffuse rather than direct radiation. Leaves at different heights in the canopy are on different portions of the light response curve, which Friend demonstrates lead to 20–30% greater daytime canopy NPP with no change in night-time NPP. This contrasts with the response in this study from increasing N_{10} , which increased daytime NPP and decreased night-time NPP (through increased autotrophic respiration).

It is unlikely that including soil respiration in the optimisation (through soil carbon content, C_s , in Table 1) would have produced a more satisfactory calibration. A lower value of C_s would have decreased daytime soil respiration and NEE, and allowed a lower calibrated value of V_{\max} in order to simulate the observed daytime carbon uptake. However, mean modelled soil respiration at $0.30 \times 10^{-7} \text{ kgC m}^{-2} \text{ s}^{-1}$ was already lower than an observed value of $0.78 \times 10^{-7} \text{ kgC m}^{-2} \text{ s}^{-1}$ for forest in this area (Araújo et al., 2002). So modelled soil respiration may have been degraded to simulate the available observations of NEE. This reflects a more general requirement for concurrent observations of NEE, soil respiration and within-canopy CO_2 storage in order to more rigorously validate models.

When the revised soil parameters were used total soil moisture content at C14 was higher than with the default soil parameters, even though the

plant available water content was reduced from 966 mm to 327 mm. This was due to a combination of reduced transpiration through soil moisture stress and an increase in field capacity from 814 mm to 976 mm. Substantial soil moisture stresses were simulated for both sites when the revised parameters were used even though rainfall was average at C14 and above average at K34. To some extent, rainfall in the preceding year is more important because it defines how much soil moisture recharge is needed from rainfall in the study year. At a rainforest site near Marabá in Pará, Hodnett et al. (1996a) observed that the soil profile did not always wet-up to the same level through each wet season, and this led to lower evaporation rates in the succeeding dry season. Simulations were initialised with saturated soils but soil moisture fell rapidly to near field capacity in all runs. The observed soil moisture contents of about 1100–1200 mm could not have been simulated because this was greater than the modelled field capacity. It is likely that because of root depth and usage the forest responds in a more complex way than is currently represented by the model. Desborough (1997) and Zeng et al. (1998) demonstrate that vertical root distribution in a SVAT has a significant impact on modelled transpiration. Greater consideration of this feature may be required to accurately simulate the forest response to soil moisture status.

Observed annual NEE is estimated to be $-5.9 \text{ tC ha}^{-1} \text{ yr}^{-1}$ at C14 (Malhi et al., 1998) and $-7.7 \pm 0.25 \text{ tC ha}^{-1} \text{ yr}^{-1}$ at K34 (Araújo et al., 2002). The C14 value was calculated from CO_2 flux data prior to reanalysis for low-frequency transport. However, Malhi et al. (2002) found that the reanalysis increased the magnitude of both day and night-time fluxes, which led to a negligible change in the net carbon balance. Estimates of annual NEE from previous studies were more conservative with $-2.2 \text{ tC ha}^{-1} \text{ yr}^{-1}$ at Reserva Ducke, Manaus (Fan et al., 1990) and $-1.0 \text{ tC ha}^{-1} \text{ yr}^{-1}$ at Reserva Jaru, Rondônia (Grace et al., 1995). These estimates were based on short datasets of 12 and 55 days respectively, whereas the C14 and K34 estimates were based on much longer periods of 243 and 365 days respectively. Before calibration, annual NEE modelled by MOSES was $+0.20 \text{ tC ha}^{-1} \text{ yr}^{-1}$ at C14 and $+0.24 \text{ tC ha}^{-1} \text{ yr}^{-1}$ at K34, closer to equilibrium than observations suggest. It is likely that

observations at most tropical forest sites are over-estimating net carbon uptake due to problems with the eddy-covariance technique in stable conditions and horizontal transport of CO₂ within the canopy airspace (Malhi et al., 2002). MOSES-modelled values after calibration were $-0.76 \text{ t C ha}^{-1} \text{ yr}^{-1}$ and $+1.8 \text{ t C ha}^{-1} \text{ yr}^{-1}$ for the C14 and K34 sites respectively. Although daytime carbon uptake increased upon calibration, plant respiration also increased, leading to greater night-time fluxes from land to atmosphere. The net effect was to keep the overall modelled carbon balance relatively close to equilibrium.

The observed rate of CO₂ uptake at C14 was persistently greater than at K34 due to physical differences between the sites. It is unsurprising that this difference was not captured by MOSES because a similar site description (root depth, soil parameters, vegetation height, etc.) was used for both sites. However, errors in the uncalibrated model diurnal cycle of NEE were sufficient that the calibration against C14 flux data greatly improved the simulation of CO₂ fluxes at both sites.

Botta et al. (2002), using a terrestrial ecosystem model, found that the carbon balance of Amazonia between 1935 and 1995 varied with time-scales of 3–4, 8–9 and 24–28 years in response to climate variability. This resulted in the modelled Amazonian carbon balance going through a sequence of neutral, net source, net sink, neutral through the last century. As a result, they advise caution when inferring long-term estimates of Amazonian carbon balance from relatively short-term observation periods. However, this does not detract from the use of these data for assessing process-based models, as in this study. Indeed, the ability to simulate available observations is an important validation of such land-surface and ecosystem models, as data are not available to corroborate the results from longer simulations.

6. Conclusions

This study has shown that the land-surface model MOSES is able to simulate the observed fluxes of heat, moisture and carbon for two central Amazonian forest sites with reasonable accuracy. Persistent stomatal closure between 1000 and 1500 hours led to underprediction of the maximum daytime carbon uptake and a high Bowen ratio.

These problems were remedied through calibration of four parameters in the conductance-photosynthesis sub-model, including leaf nitrogen content. It was found that errors in the diurnal cycles of carbon and water vapour flux were due to saturation of the response to solar radiation at low light levels. An increased rate of daytime photosynthesis was achieved at the expense of degrading modelled long-term moisture and heat fluxes. There was little change to the modelled net carbon balance upon calibration due to an increase in night-time respiration as well as daytime photosynthesis due to greater leaf nitrogen content. The parameters calibrated at C14 were applied with success at K34, which suggests that they are not overly site specific. This is important if the response of a land-surface model, calibrated against relatively few sites, is to be generalised for use in GCMs.

Seasonality in the observed fluxes due to soil moisture change was not simulated well by MOSES. Applying more realistic soil parameters reduced the amount of moisture available for transpiration and led to a reduction in canopy conductance due to water stress at the end of the dry season. However, water stress simulated at K34 during a period of plentiful rainfall, and during the wet season at C14, indicated that consideration of the below-ground hydrology is needed beyond soil hydraulic parameters. For example, properties of the forest such as root depth and root usage.

Confidence in GCM simulations of future climate, where Amazonia is predicted to become drier, is dependent on the accuracy of the land-surface models response to low soil moisture. Existing datasets of carbon and water fluxes for Amazonian rainforest probably do not cover a sufficient range of soil moisture conditions to allow this response to be established confidently. Data are needed spanning longer periods and ideally through El Niño cycles, which is the principal mode of interannual rainfall variability in this region.

Acknowledgements

This modelling work was funded by Natural Environment Research Council non-thematic grant GR3/12967. The authors thank Richard Harding, Douglas Clark and two anonymous referees for their comments on an early draft.

References

- Araújo A, Nobre A, Kruijt B, Elbers J, Dallarosa R, Stefani P, von Randow C, Manzi A, Culf A, Gash J, Valentini R, Kabat P (2002) Comparative measurements of carbon dioxide fluxes from two nearby towers in central Amazonian rainforest: The Manaus LBA site. *J Geophys Res* 107: 8061
- Bastidas L, Gupta H, Sorooshian S, Shuttleworth W, Yang Z (1999) Sensitivity analysis of a land surface scheme using multicriteria methods. *J Geophys Res* 104(D16): 19481–19490
- Betts R, Cox P, Collins M, Harris P, Huntingford C, Jones C (2004) The role of ecosystem-atmosphere interactions in simulated Amazonian precipitation decrease and forest dieback under global climate warming. *Theor Appl Climatol* (in press)
- Botta A, Ramankutty N, Foley J (2002) Long-term variations in climate and carbon fluxes over the Amazon basin. *Geophys Res Lett* 29(9): 33-1–33-4
- Campbell G (1974) A simple method for determining unsaturated conductivity from moisture retention data. *Soil Sci* 117: 311–314
- Collatz G, Ball J, Grivet C, Berry J (1991) Physiological and environmental regulation of stomatal conductance, photosynthesis and transpiration: a model that includes a laminar boundary layer. *Agric Forest Meteorol* 54: 107–136
- Collatz G, Ribas-Carbo M, Berry J (1992) Coupled photosynthesis-stomatal conductance model for leaves of C_4 plants. *Aust J Plant Physiol* 19: 519–538
- Correa J (1984) Características físico hídricas dos solos latossolo amarelo, podzólico vermelho amarelo e podzol hidromórfico do estado do Amazonas. *Pesquisa Agropecuária Brasileira* 20: 1317–1322
- Cox P, Betts R, Bunton C, Essery R, Rowntree P, Smith J (1999) The impact of new land surface physics on the GCM simulation of climate and climate sensitivity. *Clim Dyn* 15: 183–203
- Cox P, Betts R, Collins M, Harris P, Huntingford C, Jones C (2004) Amazonian rainforest dieback and climate-carbon cycle projections for the 21st century. *Theor Appl Climatol* (in press)
- Cox P, Betts R, Jones C, Spall S, Totterdell I (2000) Acceleration of global warming due to carbon-cycle feedbacks in a coupled climate model. *Nature* 408: 184–187
- Delire C, Foley J (1999) Evaluating the performance of a land-surface/ecosystem model with biophysical measurements from contrasting environments. *J Geophys Res* 104: 16895–16909
- Desborough C (1997) The impact of root weighting on the response of transpiration to moisture stress in land surface schemes. *Mon Wea Rev* 125: 1920–1930
- Dirmeyer P, Shukla J (1994) Albedo as a modulator of climate response to tropical deforestation. *J Geophys Res* 99(D10): 20863–20877
- Essery R, Best M, Cox P (2001) MOSES 2.2 Technical Documentation. Tech. rep. Met Office
- Fan SM, Wofsy S, Bakwin P, Jacob D, Fitzjarrald D (1990) Atmosphere-Biosphere exchange of CO_2 and O_3 in the Central Amazon forest. *J Geophys Res* 95(D10): 16851–16864
- Friedlingstein P, Bopp L, Cias P, Dufrense JL, Fairhead L, LeTruet H, Monfray P, Orr J (2001) Positive feedback between future climate change and the carbon cycle. *Geophys Res Lett* 28(8): 1543–1546
- Friend A (2001) Modelling canopy CO_2 fluxes: are ‘big-leaf’ simplifications justified? *Glob Ecol Biogeog* 10: 603–619
- Friend A, Stevens A, Knox R, Cannell M (1997) A process-based terrestrial biosphere model of ecosystem dynamics (Hybrid v3.0). *Ecol Model* 95: 249–287
- Garratt J (1993) Sensitivity of climate simulations to land-surface and atmospheric boundary-layer treatments – A review. *J Climate* 6: 419–449
- van Genuchten M (1980) A closed-form equation for predicting the hydraulic conductivity of unsaturated soils. *Soil Sci Soc Am J* 44: 892–898
- Grace J, Lloyd J, McIntyre J, Miranda A, Meir P, Miranda H, Moncrieff J, Massheder J, Wright I, Gash J (1995) Fluxes of carbon dioxide and water vapour over an undisturbed tropical forest in south-west Amazonia. *Glob Chan Biol* 1: 1–12
- Harris P, Huntingford C, Cox P, Gash J, Malhi Y (2004) Effect of soil moisture on canopy conductance of Amazonian rainforest. *Agric For Meteorol* (in press)
- Hodnett M, Oyama M, Tomasella J, Marques Filho O (1996a) Comparisons of long-term soil water storage behaviour under pasture and forest in three areas of Amazonia. In: Gash J, Nobre C, Roberts J, Victoria R (eds) Amazonian deforestation and climate. Chichester: Wiley, chap 3, pp 57–78
- Hodnett M, Tomasella J, Marques Filho O, Oyama M (1996b) Deep soil water uptake by forest and pasture in central Amazonia: predictions from long term daily rainfall data using a simple water balance model. In: Gash J, Nobre C, Roberts J, Victoria R (eds) Amazonian deforestation and climate. Chichester: Wiley, chap 4, pp 79–100
- Jacobs C (1994) Direct impact of atmospheric CO_2 enrichment on regional transpiration Ph.D. thesis Wageningen Agricultural University
- Lean J, Bunton C, Nobre C, Rowntree P (1996) The simulated impact of Amazonian deforestation on climate using measured ABRACOS vegetation characteristics. In: Gash J, Nobre C, Roberts J, Victoria R (eds) Amazonian deforestation and climate. Chichester: Wiley, chap 31, pp 549–576
- Lenard R, Parker J, Mishra S (1989) On the correspondence between Brooks-Corey and van Genuchten models. *J Irrigat Drain Engin* 115: 744–751
- Malhi Y, Grace J (2000) Tropical forests and carbon dioxide. *Trends Ecol Evol* 15(8): 332–337
- Malhi Y, Nobre A, Grace J, Kruijt B, Pereira M, Culf A, Scott S (1998) Carbon dioxide transfer over a Central Amazonian rainforest. *J Geophys Res* 103(D24): 31593–31612
- Malhi Y, Pegoraro E, Nobre A, Pereira M, Grace J, Culf A, Clement R (2002) Energy and water dynamics of a central Amazonian rain forest. *J Geophys Res* 107(D20): 45-1–45-17

- Monteith J (1965) Evaporation and environment. *Symp Soc Exp Biol* 19: 205–224
- Morel-Seytoux H, Meyer P, Nachabe M, Touma J, van Genuchten M, Lenard R (1996) Parameter equivalence for the Brooks-Corey and van Genuchten soil characteristics: preserving the effective capillary drive. *Water Resour Res* 32: 849–851
- Nepstad D, de Carvalho C, Davidson E, Jipp P, Lefebvre P, Negreiros G, da Silva E, Stone T, Trumbore S, Vieira S (1994) The role of deep roots in the hydrological and carbon cycles of Amazonian forests and pastures. *Nature* 372: 666–669
- Polcher J (1995) Sensitivity of tropical convection to land-surface processes. *J Atmos Sci* 52(17): 3143–3161
- von Randow C, Manzi A, Kruijt B, de Oliveira P, Zanchi F, Silva R, Hodnett M, Gash J, Elbers J, Waterloo M, Cardoso F, Kabat P (2004) Comparative measurements and seasonal variations in energy and carbon exchange over forest and pasture in Central West Amazonia. *Theor Appl Climatol* (in press)
- Roberts J, Cabral O, da Costa J, McWilliam AL (1996) An overview of the leaf area index and physiological measurements during ABRACOS. In: Gash J, Nobre C, Roberts J, Victoria R (eds) *Amazonian deforestation and climate*. Chichester: Wiley, chap 16, pp 287–306
- da Rocha H, Sellers P, Collatz G, Wright I, Grace J (1996) Calibration and use of the SiB2 model to estimate water vapour and carbon exchange at the ABRACOS forest sites. In: Gash J, Nobre C, Roberts J, Victoria R (eds) *Amazonian deforestation and climate*. Chichester: Wiley, chap 27, pp 459–471
- Sellers P, Dickinson R, Randall D, Betts A, Hall F, Berry J, Collatz G, Denning A, Mooney H, Nobre C, Sato N, Field C, Henderson-Sellers A (1997) Modelling the exchanges of energy, water, and carbon between continents and the atmosphere. *Science* 275: 502–509
- Sellers P, Mintz Y, Sud Y, Dalcher A (1992) A simple biosphere model (SiB) for use within general circulation models. *J Atmos Sci* 43: 505–531
- Sen O, Shuttleworth W, Yang ZL (2000) Comparative evaluation of BATS2, BATS, and SiB2 with Amazon data. *J Hydromet* 1: 135–153
- Shuttleworth W (1988) Evaporation from Amazonian rain-forest. *Proc R Soc Lond Ser B* 233: 321–346
- Shuttleworth W (1989) Micrometeorology of temperate and tropical forest. *Philos Trans Roy Soc London Ser B* 324: 299–334
- Sommer R, Sá TdA, Vielhauer K, de Araújo A, Fölster H, Vlek P (2002) Transpiration and canopy conductance of secondary vegetation in the eastern Amazon. *Agric Forest Meteorol* 112: 103–121
- White A, Cannell M, Friend A (1999) Climate change impacts on ecosystems and the terrestrial carbon sink: a new assessment. *Glob Environ Change* 9: S21–S30
- Williams M, Malhi Y, Nobre A, Rastetter E, Grace J, Pereira M (1998) Seasonal variation in net carbon exchange and evapotranspiration in a Brazilian rain forest: a modelling analysis. *Plant Cell Environ* 21: 953–968
- Wright I, Nobre C, da Rocha H, Roberts J, Vertamatti E, Culf A, Santos-Alvala R, Hodnett M, Ubarana V (1996) Towards a GCM parameterization for Amazonia. In: Gash J, Nobre C, Roberts J, Victoria R (eds) *Amazonian deforestation and climate*. Chichester: Wiley, chap 28, pp 473–504
- Zeng X, Dai YJ, Dickinson R, Shaikh M (1998) The role of root distribution for climate simulation over land. *Geophys Res Lett* 24(24): 4533–4536

Authors' addresses: P. P. Harris (e-mail: ppha@ceh.ac.uk), C. Huntingford, J. H. C. Gash and M. G. Hodnett, Centre for Ecology and Hydrology, Wallingford, OX10 8BB, U.K.; P. M. Cox, Hadley Centre for Climate Prediction and Research, Met Office, Exeter, EX1 3PB, U.K.; Y. Malhi, Ecology and Resource Management, School of GeoSciences, University of Edinburgh, Edinburgh, EH9 3JU, U.K.; A. C. Araújo, Instituto Nacional de Pesquisas da Amazonia, Manaus, Amazonas, Brazil.